

## **Fabrication and local laser heating of freestanding Ni<sub>80</sub>Fe<sub>20</sub> bridges with Pt contacts displaying anisotropic magnetoresistance and anomalous Nernst effect**

F. Brandl and D. Grundler

Citation: [Applied Physics Letters](#) **104**, 172401 (2014); doi: 10.1063/1.4874302

View online: <http://dx.doi.org/10.1063/1.4874302>

View Table of Contents: <http://scitation.aip.org/content/aip/journal/apl/104/17?ver=pdfcov>

Published by the [AIP Publishing](#)

---

### **Articles you may be interested in**

[Anisotropy in collective precessional dynamics in arrays of Ni<sub>80</sub>Fe<sub>20</sub> nanoelements](#)

*J. Appl. Phys.* **111**, 07D503 (2012); 10.1063/1.3672402

[Large enhancement of anisotropic magnetoresistance and thermal stability in Ta/NiFe/Ta trilayers with interfacial Pt addition](#)

*Appl. Phys. Lett.* **96**, 092509 (2010); 10.1063/1.3334720

[Modulation of magneto-resistance with measurement current in patterned Ni<sub>80</sub>Fe<sub>20</sub> wires](#)

*J. Appl. Phys.* **97**, 10J708 (2005); 10.1063/1.1854071

[Effect of contact geometry on the magnetoresistance response of Ni<sub>80</sub>Fe<sub>20</sub> antidot array](#)

*J. Appl. Phys.* **97**, 10J902 (2005); 10.1063/1.1853751

[Current induced magnetic switching in Ni<sub>80</sub>Fe<sub>20</sub>, Ni, Fe, and Co wires](#)

*J. Appl. Phys.* **97**, 10C711 (2005); 10.1063/1.1853237

---



**NEW! Asylum Research MFP-3D Infinity™ AFM**  
Unmatched Performance, Versatility and Support

**OXFORD INSTRUMENTS**  
*The Business of Science®*

Stunning high performance

Simpler than ever to GetStarted™

Comprehensive tools for nanomechanics

Widest range of accessories for materials science and bioscience

*Asylum Research*

# Fabrication and local laser heating of freestanding $\text{Ni}_{80}\text{Fe}_{20}$ bridges with Pt contacts displaying anisotropic magnetoresistance and anomalous Nernst effect

F. Brandl and D. Grundler<sup>a)</sup>

*Lehrstuhl für Physik funktionaler Schichtsysteme, Physik-Department E10, Technische Universität München, James-Frank-Str. 1, D-85748 Garching b. München, Germany*

(Received 26 January 2014; accepted 21 April 2014; published online 30 April 2014)

In spin caloritronics, ferromagnetic samples subject to relatively large in-plane temperature gradients  $\nabla T$  have turned out to be extremely interesting. We report on a preparation technique that allows us to create freely suspended permalloy/Pt hybrid structures where a scanning laser induces  $\nabla T$  on the order of a few  $\text{K}/\mu\text{m}$ . We observe both the anisotropic magnetoresistance at room temperature and the magnetic field dependent anomalous Nernst effect under laser heating. The technique is promising for the realization of device concepts considered in spin caloritronics based on suspended ferromagnetic nanostructures with electrical contacts. © 2014 AIP Publishing LLC. [<http://dx.doi.org/10.1063/1.4874302>]

The generation of a pure spin current without the net flow of charge is of great interest especially for future logical devices with low power consumption. The spin-Seebeck effect (SSE) addressed by Uchida *et al.*<sup>1</sup> in 2008 further fueled this research direction in spintronics.<sup>2–4</sup> It was reported that an in-plane temperature gradient  $\nabla T$  in the ferromagnet permalloy  $\text{Ni}_{80}\text{Fe}_{20}$  (Py) generated a pure spin current that flowed collinearly to  $\nabla T$ .<sup>1</sup> The spin current was not directly measured. Instead, a thin platinum (Pt) stripe was attached to the ferromagnet orientated perpendicular to the temperature gradient. The current was argued to enter Pt and provoke to a charge imbalance (electric voltage) via the inverse spin Hall effect (ISHE)<sup>5–7</sup> exploiting the large spin-orbit coupling in Pt. The microscopic origin of the reported spin current in this so-called transverse SSE (TSSE) configuration is under intense investigation<sup>8</sup> and, e.g., phonons in the substrate have been argued to play a role.<sup>9–13</sup> Accordingly, experiments were conducted where bulk substrates were replaced by thin membranes supporting Py.<sup>14</sup> In membrane-supported Py, the TSSE was not resolved. Still, freestanding Py with Pt contacts has not yet been realized due to severe experimental challenges when preparing air bridges of a thin ferromagnet with similarly thin voltage probes. Beyond TSSE, such freestanding Py and the corresponding preparation technology would be of great interest for further experiments in spin caloritronics.<sup>15</sup> Here, an in-plane temperature gradient in a ferromagnet is key and a heat sink provided by a substrate needs to be avoided locally. Examples are ferromagnetic nanomachines predicted in Refs. 16 and 17 and the magnetic Seebeck effect reported for an insulating ferrimagnet.<sup>18</sup>

In this work, we report a preparation technology for freestanding Py bridges equipped with Pt stripes (Fig. 1). The magnetic hysteresis of the suspended device was explored by the anisotropic magnetoresistance (AMR) effect in in-plane fields  $H$ . Using a scanning laser setup, we generated local temperature gradients. We found magnetothermal

signals consistent with Seebeck and anomalous Nernst effect (ANE) voltages similar to experiments performed on bulk samples in Refs. 19 and 20. Our data suggested an in-plane temperature gradient on the order of  $10\text{K}/\mu\text{m}$ . For rotated  $H$ , the angular dependent voltages measured on Pt stripes did not agree with the behavior expected for the TSSE, but were consistent with a remaining ANE contribution. The observation of both AMR and ANE makes the developed preparation technique attractive for freestanding Pt/Py hybrid structures optimized for further spin caloritronics experiments.<sup>16–18</sup>

For preparing suspended Py, we followed the concept of metallic air bridges established in semiconductor technology for isolated gate electrodes.<sup>21</sup> For this, a thin-film stripe was underetched locally in a final preparation step. As most wet-chemical etchants attacked Py, a specific protection scheme based on thin aluminium (Al) was developed. For the substrate, we used gallium arsenide (GaAs). In a first step, the substrate was coated with a 21 nm thick Al film. Then, Pt stripes were predefined by 5- $\mu\text{m}$ -wide trenches produced by photolithography. In the trenches, the 21-nm-thick aluminum was completely etched away by a standard photo-resist developer. The etched Al regions were then refilled with 6 nm thick Al and 15 nm thick Pt in order to get Pt stripes embedded in Al as shown in Fig. 1(a). In a next step, the 10- $\mu\text{m}$ -wide Py stripe was defined by photolithography. We deposited 40-nm-thick polycrystalline Py by electron-beam evaporation after precleaning the surface of Pt using *in situ* ion milling. We performed lift-off processing with one-and-the-same resist mask. Two small windows were opened in the Al next to the Py stripe [Fig. 1(b)] using a photo-resist mask and standard photo-resist developer after the relevant UV light exposure. The windows in Al allowed us to etch the underlying GaAs with an isotropic etchant (citric acid and  $\text{H}_2\text{O}_2$ ) such that the Py/Pt hybrid structure was underetched and separated from the GaAs substrate material [Fig. 1(c)]. The initial bottom layer of Al was key to protect both Py and Pt against the wet etchant. In a last step, we removed the resist and Al of the freestanding segment in acetone and a short dip of standard photo-resist developer, respectively. A freestanding bridge of

<sup>a)</sup>grundler@ph.tum.de

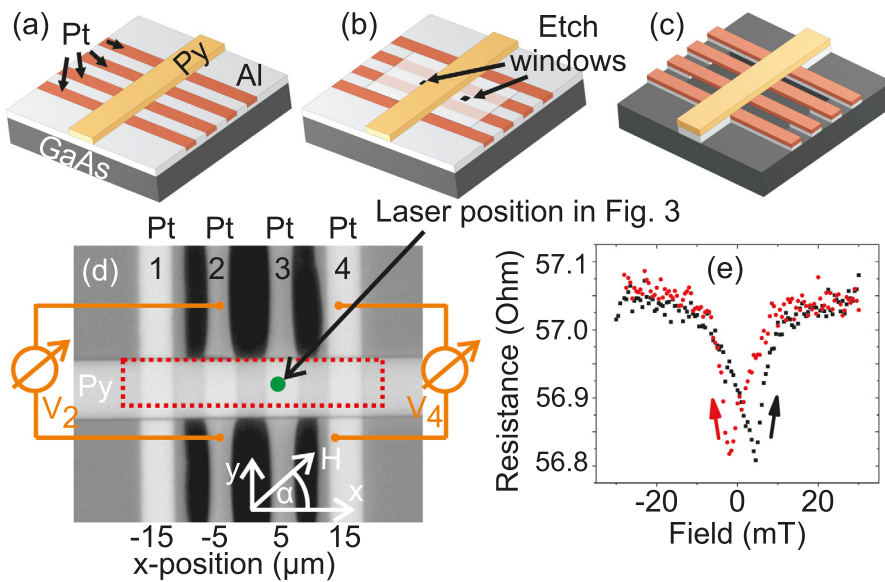


FIG. 1. (a) Pt leads embedded in an Al thin film underneath Py. (b) GaAs is etched isotropically through two windows in Al. (c) Final sample. (d) Microscopy image (top view) with contact configuration and coordinate system. The 40 nm thick Py stripe is 10  $\mu\text{m}$  wide and crossed by four 15 nm thick and 5  $\mu\text{m}$  wide Pt stripes. Between leads 1 and 4, the hybrid structure is underetched (black). (e) Magnetic field dependent resistance  $R$  measured between leads 1 and 4.  $\mu_0 H$  is varied in steps of 0.5 mT and applied along the current-biased Py stripe.

Py and Pt remained [Fig. 1(d)]. The ultrasonic agitation was performed only at small power level to minimize the number of cracks. Nevertheless, contacts sometimes broke. A critical point dryer might enlarge the yield by avoiding surface tension effects when drying the sample after the final wet-etching step. We fabricated a reference Py/Pt hybrid structure directly on a GaAs substrate without underetching. Additionally, a suspended Py/Pt hybrid structure was prepared using a silicon-on-insulator substrate where we removed the silicon device layer during the preparation process (not shown). Samples were mounted in a room temperature set up providing an in-plane magnetic field  $\mathbf{H}$  under different angles  $\alpha$ . The magnetoresistance  $R(H)$  was measured between Pt stripes using the lock-in technique with a current amplitude  $I$  of 100 nA applied to the Py stripe. To generate temperature gradients, we made use of a laser-heating setup with a focused laser of a wavelength of 532 nm (Fig. 2). Thereby, we followed an approach introduced to spin caloritronics at an early stage by Gravier *et al.*<sup>22</sup> and recently revisited by further groups.<sup>19,20,23,24</sup> We positioned the laser spot with an accuracy of several tens of nm on the sample using markers, an objective (100 $\times$  Mitutoyo Plan APO SL) and a camera combined with a commercially available software (TFPDAS4-MICRO). The focus was adjusted automatically using the signal of a photodiode behind a pinhole. The laser spot diameter of 1.1  $\mu\text{m}$  was determined by driving the laser over a sharp edge and measuring the reflected light intensity (10%/90% criterion). We modulated the laser intensity at 171 Hz to detect laser-induced voltages phase-sensitively using contacts as shown in Fig. 1(d). The whole optics is mounted on a nanopositioning system (Aerotech ANT130-060-XY-PLUS) to keep the sample at a fixed position in the center of the field coils.

Figure 1(e) shows  $R(H)$  probed without laser illumination when  $\mathbf{H}$  is collinear with the Py stripe. The hysteretic behavior is attributed to the AMR effect. At large  $|H|$ , the magnetization  $\mathbf{M}$  of the stripe is collinear with  $I$  providing a large resistance  $R_{\text{max}}$ . When approaching  $H=0$ , the resistance value decreases indicating that due to domain formation and rotation of  $\mathbf{M}$  magnetic moments deviate from the current direction.

From the field position of the minimum  $R_{\text{min}}$ , the coercive field is estimated to be about 3 mT. This value is slightly smaller compared to the value observed in Fig. 2(b) of Ref. 20. There, Py from the same evaporation chamber was used and deposited on a bulk substrate of MgO.  $R(H)$  of Fig. 1(e) varies between  $R_{\text{min}} = 56.80 \Omega$  and  $R_{\text{max}} = 57.05 \Omega$  providing a magnetoresistance (MR) ratio  $\Delta R/R = (R_{\text{max}} - R_{\text{min}})/R_{\text{max}}$  of 0.44%. This value is larger by a factor of two compared to Ref. 20. The small coercive field and relatively large MR ratio substantiate that the involved preparation technique used here

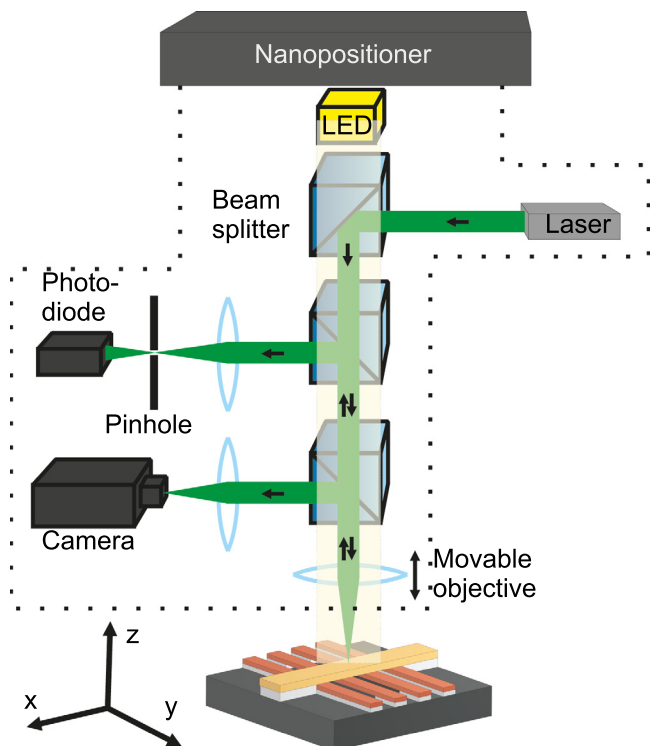


FIG. 2. The scanning laser light is focussed by an objective on the fixed sample illuminated by a LED. For position and focus control, the reflected light is transmitted to a camera and a photodiode with a pinhole.

did not deteriorate the quality of the magnetic thin film. Via  $\rho_{\text{Py}} = R_{\text{max}} \times (wt)/l$  we calculate the specific resistance of Py to be  $\rho_{\text{Py}} = 9 \times 10^{-5} \Omega \text{cm}$  ( $w = 10 \mu\text{m}$ : width of Py,  $t = 40 \text{nm}$ : thickness of Py,  $l = 25 \mu\text{m}$ : length between Pt leads 1 and 4).<sup>25</sup> The value is comparable to Ref. 26. The shape anisotropy field of the Py stripe is calculated to be  $\mu_0 N_y M_S \approx 2.5 \text{ mT}$ , where  $N_y = 2t/(\pi w)$  is the relevant component of the demagnetization tensor<sup>27</sup> and  $\mu_0 M_S \approx 1 \text{ T}$  is the saturation magnetization of Py. As  $R(H)$  equals  $R_{\text{max}}$  for  $\mu_0 |H| > 20 \text{ mT}$ , we consider the magnetization of the Py stripe to be saturated for the field of 70 mT used later.

For Fig. 3(a), we scanned the laser with a power of about 8 mW over the structure similar to Ref. 20. The laser-induced voltages are recorded at  $I = 0$  and  $H = 0$ . The position  $(x, y) = (0, 0)$  represents the center of the suspended region. We find large absolute voltages when the laser resides on the region where lead 2 contacts the Py stripe (contact region). From positive to negative  $y$ , the voltage sign changes in a similar manner as in Ref. 20. We attribute the observed voltage to the Seebeck effect. It occurs when the upper and lower edges of the contact region are at different temperatures. Positioning the laser spot at  $x = -5 \mu\text{m}$  and  $y = 5 \mu\text{m}$ , we obtain the maximum voltage of  $140 \mu\text{V}$ . To evaluate the relevant temperature  $T$ , we assume an effective Seebeck coefficient  $S_{\text{eff}}$  for the contact region following Ref. 20. The coefficient is calculated to be  $S_{\text{eff}} = (\sigma_{\text{Pt}} S_{\text{Pt}} + \sigma_{\text{Py}} S_{\text{Py}}) / (\sigma_{\text{Pt}} + \sigma_{\text{Py}}) = -6.57 \mu\text{V/K}$ , with  $\sigma_{\text{Pt}} = 9.44 \times 10^6 \text{ S/m}$ ,<sup>28</sup>  $\sigma_{\text{Py}} = \rho_{\text{Py}}^{-1} = 1.1 \times 10^6 \text{ S/m}$ ,  $S_{\text{Pt}} = -5 \mu\text{V/K}$ ,<sup>29</sup> and  $S_{\text{Py}} = -20 \mu\text{V/K}$ .<sup>30</sup> The voltage signal  $V_2$  of  $140 \mu\text{V}$  translates to a temperature difference of  $\Delta T = 140 \mu\text{V} / (S_{\text{Pt}} - S_{\text{eff}}) = 89.2 \text{ K}$  across the width of the Py stripe. To estimate the lateral temperature gradient in the contact region along the  $y$ -direction, we assume a linear temperature variation over the  $10 \mu\text{m}$  wide Py stripe and  $T$  being close to room temperature at the bottom edge. We obtain  $\nabla T \approx 9 \text{ K}/\mu\text{m}$ . The gradient in the  $x$ -direction is expected to be of the same order as the GaAs substrate under lead 1 (and 4) acts as an efficient heat sink at room temperature. It is also  $10 \mu\text{m}$  away from the laser position where  $V_2 = 140 \mu\text{V}$

measured. Note that this gradient in  $x$ -direction would be even larger than  $9 \text{ K}/\mu\text{m}$  if the bottom edge of the contact region was at larger  $T$  than room temperature. We thereby create temperature gradients being large enough to generate spin caloric transport effects.<sup>1,31,32</sup>

In Fig. 3(b), we show the voltage  $V_2$  recorded at lead 2 while the magnetic field angle  $\alpha$  is varied ( $\mu_0 H = 70 \text{ mT}$ ). The position of the laser spot during the measurement is fixed at the center of lead 3 [dot in Fig. 1(d)] to minimize the Seebeck voltage [compare Fig. 3(a)]. At the same time, we generate a temperature gradient in the  $x$ -direction of the same order as evaluated above. The measured voltage signal shows a sine-like dependence as it would be expected from the TSSE.<sup>1</sup> The maximum values are found at  $\alpha = (n + 1) \times 180^\circ$  with  $n = -2, 0, 2$ . Here, the magnetic field is collinear with the Py stripe. The fitting procedure using a sine curve provides an amplitude of  $19 \text{ nV}$  and an offset voltage of  $-11 \text{ nV}$ . We attribute the offset to a remaining Seebeck effect and a photovoltage as the substrate (GaAs) is a direct band-gap semiconductor.<sup>24,33</sup> In Fig. 3(c), we show the voltage detected at lead 4 while the laser spot is at the same position as in (b). Using lead 4 the in-plane temperature gradient is of opposite sign compared to Fig. 3(b). The amplitude of the sine function amounts to  $23 \text{ nV}$  with a voltage offset of  $439 \text{ nV}$ . Assuming the TSSE, one would expect that the sine function should be shifted by  $180^\circ$  compared to (b). This shift is however not observed. This finding rules out the TSSE, similar to experiments performed with ferromagnets on thin membranes.<sup>14,34</sup> Due to the observed symmetry, the planar Nernst effect<sup>14,34</sup> is excluded. We attribute the voltage variation with  $\alpha$  to the anomalous Nernst effect<sup>35</sup> induced by a remaining out-of-plane temperature gradient in the Py stripe. This gradient is expected to occur in the contact region where the Pt lead provides a heat sink on the lower side of the Py compared to the upper Py side that is in air. Considering an anomalous Nernst coefficient  $S_{N,\text{Py}} = R_N \times S_{\text{Py}}$  with  $R_N = 0.13$  (Ref. 36), the temperature difference across the  $40 \text{ nm}$  thick Py stripe is  $7 \text{ mK}$  ( $9 \text{ mK}$ ) for the measured amplitude of  $19 \text{ nV}$  ( $23 \text{ nV}$ ). Measurements on the further Pt stripes with varying laser position and field angle showed similar behavior. A free-standing  $65 \text{ nm}$  thick Py bridge with  $15 \text{ nm}$  thick Pt contacts prepared on a silicon-on-insulator substrate was explored with a focused laser of a wavelength of  $407 \text{ nm}$ . The data showed consistent AMR and Seebeck voltages as well as sinusoidal angle-dependent voltage variations for a rotating field of  $30 \text{ mT}$ . We detected an amplitude of  $680 \text{ nV}$  ( $950 \text{ nV}$ ) at an offset voltage of  $17.2 \mu\text{V}$  ( $46.6 \mu\text{V}$ ) while the laser spot was positioned on the left (right) side of a Pt lead crossing the Py bridge. The larger amplitude is explained by a more inhomogeneous heating of the  $65 \text{ nm}$  thick Py leading to a larger out-of-plane temperature gradient and ANE. A signature suggesting the TSSE was not identified either. The experiments on the not-underetched reference sample provided an amplitude (offset voltage) of about  $3.5 \mu\text{V}$  ( $-3.6 \mu\text{V}$ ).<sup>37</sup> These values are explained by a more pronounced ANE and photovoltages as the ferromagnet was directly attached to the substrate. Here, the substrate acted as an efficient heat sink in  $z$ -direction similar to Ref. 20 provoking a correspondingly large temperature gradient in the same direction.

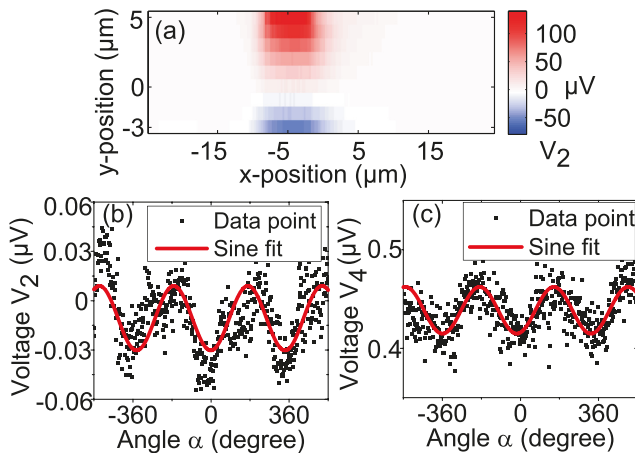


FIG. 3. (a) Color-coded voltage  $V_2$  detected with the laser positioned inside the dotted box shown in 1(d).  $x = 0$  is in the center between contacts 2 and 3. White indicates  $V = 0$ . Voltages (b)  $V_2$  and (c)  $V_4$  taken for a fixed laser position [dot in 1(d)] as a function of angle  $\alpha$  ( $\mu_0 H = 70 \text{ mT}$ ). The solid line indicates a sinusoidal dependence on  $\alpha$ .

The observation of both a spin-transport effect such as the AMR and ANE makes the suspended Py/Pt hybrid structures a promising approach for future experiments on spin caloritronic nanomachines containing tailored domain walls in suspended segments. The laser-scanning setup is based on scanning optics and a fixed sample position making rigid microwave connections to the sample possible. This feature allows for the combination of spin caloritronics with magnonics<sup>38</sup> and the exploration of the magnetic Seebeck effect in Py. The latter effect relies on an in-plane temperature gradient and has so far been reported for an insulating bulk-like ferromagnet only.<sup>18</sup>

In conclusion, we have fabricated freestanding Py stripes with Pt contacts showing soft magnetic behavior. We observed the AMR, ANE and a spatially resolved Seebeck effect using a scanning laser setup. Within the noise level, we did not find a contribution from the TSSE though a large in-plane temperature gradient on the order of a few K/ $\mu\text{m}$  was generated. The suspended devices are interesting for further spin caloritronics experiments.

We thank H. Schultheiß and acknowledge financial support through the German priority program SPP 1538 on spin caloric transport via project GR1640/5-1.

- <sup>1</sup>K. Uchida, S. Takahashi, K. Harii, J. Ieda, W. Koshibae, K. Ando, S. Maekawa, and E. Saitoh, *Nature* **455**, 778 (2008).
- <sup>2</sup>T. Yang, T. Kimura, and Y. Otani, *Nat. Phys.* **4**, 851 (2008).
- <sup>3</sup>H.-F. Lü and Y. Guo, *Appl. Phys. Lett.* **91**, 092128 (2007).
- <sup>4</sup>S. A. Wolf, D. D. Awschalom, R. A. Buhrman, J. M. Daughton, S. von Molnar, M. L. Roukes, A. Y. Chtchelkanova, and D. M. Treger, *Science* **294**, 1488 (2001).
- <sup>5</sup>E. Saitoh, M. Ueda, H. Miyajima, and G. Tatara, *Appl. Phys. Lett.* **88**, 182509 (2006).
- <sup>6</sup>T. Kimura, Y. Otani, T. Sato, S. Takahashi, and S. Maekawa, *Phys. Rev. Lett.* **98**, 156601 (2007).
- <sup>7</sup>O. Mosendz, J. E. Pearson, F. Y. Fradin, G. E. W. Bauer, S. D. Bader, and A. Hoffmann, *Phys. Rev. Lett.* **104**, 046601 (2010).
- <sup>8</sup>S. Y. Huang, X. Fan, D. Qu, Y. P. Chen, W. G. Wang, J. Wu, T. Y. Chen, J. Q. Xiao, and C. L. Chien, *Phys. Rev. Lett.* **109**, 107204 (2012).
- <sup>9</sup>C. M. Jaworski, J. Yang, S. Mack, D. D. Awschalom, J. P. Heremans, and R. C. Myers, *Nature Mater.* **9**, 898 (2010).
- <sup>10</sup>C. M. Jaworski, J. Yang, S. Mack, D. D. Awschalom, R. C. Myers, and J. P. Heremans, *Phys. Rev. Lett.* **106**, 186601 (2011).
- <sup>11</sup>J. Xiao, G. E. W. Bauer, K. Uchida, E. Saitoh, and S. Maekawa, *Phys. Rev. B* **81**, 214418 (2010).
- <sup>12</sup>K. Uchida, T. Ota, H. Adachi, J. Xiao, T. Nonaka, Y. Kajiwara, G. E. W. Bauer, S. Maekawa, and E. Saitoh, *J. Appl. Phys.* **111**, 103903 (2012).
- <sup>13</sup>S. Y. Huang, W. G. Wang, D. Qu, S. F. Lee, J. Kwo, and C. L. Chien, *Tech. Dig. - Int. Electron Devices Meet.* **2012**, 11.2.1.
- <sup>14</sup>A. D. Avery, M. R. Pufall, and B. L. Zink, *Phys. Rev. Lett.* **109**, 196602 (2012).
- <sup>15</sup>G. E. W. Bauer, E. Saitoh, and B. J. van Wees, *Nature Mater.* **11**, 391 (2012).
- <sup>16</sup>A. A. Kovalev and Y. Tserkovnyak, *Solid State Commun.* **150**, 500 (2010).
- <sup>17</sup>G. E. W. Bauer, S. Bretzel, A. Brataas, and Y. Tserkovnyak, *Phys. Rev. B* **81**, 024427 (2010).
- <sup>18</sup>S. D. Brechet, F. A. Vetro, E. Papa, S. E. Barnes, and J.-P. Ansermet, *Phys. Rev. Lett.* **111**, 087205 (2013).
- <sup>19</sup>M. Weiler, M. Althammer, F. D. Czeschka, H. Huebl, M. S. Wagner, M. Opel, I.-M. Imort, G. Reiss, A. Thomas, R. Gross, and S. T. B. Goennenwein, *Phys. Rev. Lett.* **108**, 106602 (2012).
- <sup>20</sup>A. von Bieren, F. Brandl, D. Grundler, and J.-P. Ansermet, *Appl. Phys. Lett.* **102**, 052408 (2013).
- <sup>21</sup>D. Grundler, *Phys. Rev. Lett.* **84**, 6074 (2000).
- <sup>22</sup>L. Gravier, S. Serrano-Guisan, F. Reuse, and J.-P. Ansermet, *Phys. Rev. B* **73**, 024419 (2006).
- <sup>23</sup>P. Möhrke, J. Rhensius, J.-U. Thiele, L. Heyderman, and M. Kläui, *Solid State Commun.* **150**, 489 (2010).
- <sup>24</sup>A. von Bieren, "Spin and heat transport in magnetic nanostructures," Ph.D. thesis (École Polytechnique Fédérale de Lausanne, 2012).
- <sup>25</sup>We neglect the shunting action of the Pt leads that are four times thinner compared to Py.
- <sup>26</sup>N. Garcia, C. Hao, L. Yonghua, M. Munoz, Y. Chen, Z. Cui, Z. Lu, Y. Zhou, G. Pan, and A. Pasa, *Appl. Phys. Lett.* **89**, 083112 (2006).
- <sup>27</sup>S. Demokritov, B. Hillebrands, and A. Slavin, *Phys. Rep.* **348**, 441 (2001).
- <sup>28</sup>NDT Resource Center, Conductivity and Resistivity Values for Misc. Materials.
- <sup>29</sup>J. P. Moore and R. S. Graves, *J. Appl. Phys.* **44**, 1174 (1973).
- <sup>30</sup>A. Slachter, F. L. Bakker, and B. J. van Wees, *Phys. Rev. B* **84**, 020412 (2011).
- <sup>31</sup>D. Qu, S. Y. Huang, J. Hu, R. Wu, and C. L. Chien, *Phys. Rev. Lett.* **110**, 067206 (2013).
- <sup>32</sup>M. Walter, J. Walowski, V. Zbarsky, M. Münzenberg, M. Schäfers, D. Ebke, G. Reiss, A. Thomas, P. Peretzki, M. Seibt, J. S. Moodera, M. Czerner, M. Bachmann, and C. Heiliger, *Nature Mater.* **10**, 742 (2011).
- <sup>33</sup>Photons can reach the substrate and provoke a photovoltage as the penetration depth of light with a wavelength of 532 nm is on the order of the thickness of the Py/Pt stack.
- <sup>34</sup>M. Schmid, S. Srichandan, D. Meier, T. Kuschel, J.-M. Schmalhorst, M. Vogel, G. Reiss, C. Strunk, and C. H. Back, *Phys. Rev. Lett.* **111**, 187201 (2013).
- <sup>35</sup>W. Nernst, *Ann. Phys.* **267**, 760 (1887).
- <sup>36</sup>A. Slachter, F. L. Bakker, J.-P. Adam, and B. J. van Wees, *Nat. Phys.* **6**, 879 (2010).
- <sup>37</sup>See supplementary material at <http://dx.doi.org/10.1063/1.4874302> for the angle-dependent voltage detected in the reference sample.
- <sup>38</sup>T. An, V. I. Vasyuchka, K. Uchida, A. V. Chumak, K. Yamaguchi, K. Harii, J. Ohe, M. B. Jungfleisch, Y. Kajiwara, H. Adachi, B. Hillebrands, S. Maekawa, and E. Saitoh, *Nature Mater.* **12**, 549 (2013).